CIMAC CONGRESS 25
ZURICH, MAY 19 – 23, 2025

2025 | 446

Ammonia: energy carrier only or well-suited sustainable fuel for large engine applications?

Fuels - Alternative & New Fuels

Nicole Wermuth, Graz University of Technology

Maximilian Malin, LEC GmbH
Marcel Lackner, LEC GmbH
Andreas Wimmer, Graz University of Technology

ABSTRACT

In order to achieve the global greenhouse gas emission reduction goals, a transition from an energy system based on fossil fuels to one based on renewable energy is crucial. The European Union will probably continue to cover a large part of its energy needs with imports from regions with abundant wind and solar energy in the future, making the transportation and storage of renewable energy highly relevant. Liquid hydrogen carriers are particularly suitable for storing large amounts of energy. Ammonia has significant advantages over hydrogen with regard to transport and handling since it can easily be liquified at ambient or sub-zero temperatures and has a higher volumetric energy density than liquefied hydrogen. Both, ammonia and hydrogen combustion in large-bore engines, gained interest in the last couple of years as an enabler for the decarbonization of hard-to-abate energy sectors. It is not clear, however, if direct use of ammonia in the engine or the cracking of ammonia into nitrogen and hydrogen and subsequent use of hydrogen in the engine will be the preferred path.

In this article, an assessment of the performance potential and the limitations for ammonia and hydrogen use in large-bore engines is carried out based on a combination of experimental evaluations on singl- cylinder research engines and 1D performance simulations. For ammonia, different combustion concepts will be considered since the emission profiles and favorable excess air ratios differ significantly between premixed combustion with pilot ignition or spark ignition on one hand and mixing controlled combustion with pilot ignition on the other hand. Hydrogen combustion will be evaluated in a spark ignition engine. The exhaust aftertreatment requirements are compared with regard to conversion efficiencies of selected exhaust components, exhaust gas temperature, and dosing needs of a reductant. Finally, the potential impacts on the engine architecture are compared and future research needs highlighted.

1 INTRODUCTION

In January 2025 the Copernicus Climate Change Service reported that in the year 2024 the annual temperature climbed to more than 1.5 °C above the pre-industrial level and that 2024 was confirmed to be the warmest year on record [1]. This highlights the urgency for global greenhouse gas (GHG) emission reductions and the necessity to set the world on the right path towards climate neutrality. National governments as well as other entities such as the International Maritime Organization (IMO) are setting targets, rules and boundary conditions for ambitious greenhouse gas emission reduction targets. The European Commission developed the 2030 Climate Target Plan [2] and further recommended to reduced net GHG emissions by 90 % of the 1990 levels by 2040 [3]. In order to achieve these goals a transition from an energy system based on fossil fuels to one based on renewable energy is crucial.

Renewable energy sources, such as solar, wind, and geothermal energy, are available in every country, unlike fossil fuels, which are concentrated in certain regions. Worldwide efforts are underway to increase the capacity of renewable energy plants. While renewable energy can be produced anywhere, cost efficiency may vary, making energy trade an inevitable scenario for the future. Germany, for example, is expected to remain an energy-importing country, but German import dependence was estimated in a 2022 study to significantly reduce in climate-neutral scenarios from 64 % in 2021 to 18 % to 33 % in 2045 [4].

The challenge has been finding a cost-effective way to transport renewable electricity over long distances to connect low-cost production sites with demand centers. One potential solution is using hydrogen as an energy carrier, which can be traded across borders in the form of molecules or raw materials like ammonia. According to a study by the International Renewable Energy Agency [5], Germany together with the rest of Europe, Japan and the Republic of Korea will be the biggest importers of hydrogen, while the biggest exporters identified in the study are North Africa, Australia, and Chile.

The key to the cost efficiency of hydrogen trade lies in scale, technologies, and other efficiencies that can reduce the cost of transporting hydrogen from low-cost production areas to high-demand areas. The conversion of hydrogen to ammonia is already commercially viable and ammonia is now widely traded and has a developed transport infrastructure (ports, ships, storage). Ammonia can also be used directly as a feedstock and fuel and does not necessarily need to be converted to hydrogen.

Ammonia has significant advantages over hydrogen with regard to transport and handling since it can easily be liquified at ambient or sub-zero temperatures and has a higher volumetric energy density than liquefied hydrogen. In a study of Smith and Mastorakos [6] it was found that for shorter distances (< 1600 km), the cost advantages of gaseous hydrogen pipeline transportation outweigh the disadvantages due to the lack of conversion processes and facilities. For intercontinental distances, the advantages of liquid ammonia transportation outweigh the cost disadvantages.

In a different systems-level study of ammonia and hydrogen for maritime transport [7], however, it was reported that hydrogen shipping requires a higher number of ships and the avoidance of rough seas since liquid hydrogen ships are susceptible to the effects of external weather conditions due to sloshing induced boil-off.

Menefee and Schwartz [8] found that round-trip efficiencies are lower for ammonia when hydrogen is the intended end product, as advantages in energy density are offset by efficiency penalties in ammonia synthesis and decomposition, but can be comparable when considering ammonia-to-power systems.

Both, ammonia and hydrogen combustion in large bore engines, gained interest in the last couple of years as an enabler for the decarbonization of hard to abate energy sectors. Considering the various aspects of fuel production, transportation and storage, as well as the conversion in the engine, it is not yet clear if direct use of ammonia in the engine or the cracking of ammonia into nitrogen and hydrogen and subsequent use of hydrogen in the engine will be the preferred path.

In this article an assessment of the performance potential and the challenges for ammonia and hydrogen use in large bore engines is carried out based on a combination of experimental evaluations on single cylinder research engines and 1D performance simulations. The exhaust aftertreatment requirements are compared with regard to conversion efficiencies of selected exhaust components, exhaust gas temperature and dosing needs of a reductant. Finally, the potential impacts on the engine architecture are compared and future research needs highlighted.

2 CARBON-FREE ENERGY CARRIERS

For the large-scale introduction of ammonia and hydrogen as energy carriers and fuel the whole lifecycle, including production, transport, storage and use, has to be thoroughly assessed.

Table 1: Fuel properties of ammonia and hydrogen in comparison to carbon-based e-fuels

Fuel	Lower heating value (gravimetric) [MJ/kg]	Lower heating value (volumetric) [MJ/l]	Laminar flame speed (stoichiometric) [m/s]	Min. ignition energy [mJ]	Autoignition temperature [K]
Drop-in e-fuel (diesel-like)	43	36	0.87	0.23	483
e-methane	50	36	0.38	0.29	868
e-methanol	19	15	0.36	0.14	712
e-ammonia (liquid, -33 °C)	20	14	0.07	8.00	930
e-hydrogen (liquid, -253 °C)	120	9	3.50	0.017	858

The physical and chemical properties of ammonia and hydrogen differ significantly from those of fossil fuels typically used in large-engine applications and also from those of other e-fuels. Table 1 provides an overview of properties for several carbon-based and carbon-free fuels relevant for large-engine applications. The combination of the fuel properties, safety considerations and techno-economic viewpoints determine the potential for a rapid uptake by the stakeholders.

2.1 Fuel production and handling

Hydrogen production via electrolysis using electric power from renewable energy sources is the first step in the production of e-fuels such as ammonia. The efficiency of state-of-the art electrolysis spans a range of approximately 60 to 80 % [9] with the potential to achieve efficiencies above 90 % in the next decade [10]. The fuel synthesis efficiency (energy input divided by the heating value of the fuel) exceeds 80 % for e-ammonia [9]. Carbon-free fuels benefit from the fact that no additional energy is required for the carbon capture process to keep carbon in a closed-loop cycle.

The efficiency of the fuel production process and the energy demand of the carbon capturing are reflected in the fuel costs, that are currently significantly higher for e-fuels than for fossil fuels [11]. Projections by the International Renewable Energy Agency, however, show a substantial decrease of e-fuel cost by 2050. While the production of e-ammonia requires more energy than hydrogen, ammonia has significant advantages over hydrogen in terms of transport and handling, as it can be easily liquefied at ambient or sub-zero temperatures and has a higher volumetric energy density than liquefied hydrogen (cf. Table 1).

Ammonia is known to be corrosive to certain materials such as brass, copper, nickel, elastomers, and plastics. Combustion of ammonia can result in the formation of nitric acid, which can attack and corrode other materials and plastics as well. While wear in direct contact with ammonia has not been observed to increase, there is a risk of increased wear through tribocorrosive mechanisms. Hydrogen, on the other hand, does not have a direct corrosive or wear-promoting effect. However, the higher amount of water vapor produced during hydrogen combustion can potentially lead to increased corrosion if not properly managed. Hydrogen does not contain carbon and lacks lubricating properties, making it the driest fuel and potentially causing increased wear in a hydrogen environment compared to other fuels. Overall, the material compatibility issue of using alternative fuels requires a careful material selection in conjunction with a material-related design for manufacturing engine components.

Since ammonia is difficult to ignite the likelihood of causing fires or explosive atmospheres in open spaces is relatively low. Ammonia is soluble in water and concentrations are expected to decrease more rapidly than other marine fuels after a spill [12]. The transport of ammonia in large gas carriers over long distances is state-of-the-art today. The first liquid hydrogen tankers have also already entered service.

If ammonia is used solely as a hydrogen carrier it has to be converted to hydrogen before further use. Ammonia dehydrogenation or cracking is a chemical process that involves the thermal decomposition of ammonia into its main components, molecular nitrogen (N_2) and

molecular hydrogen (H_2). The simplified reaction equation can be described as follows [13]:

$$2\ NH_{3(g)} \rightleftharpoons 3\ H_{2(g)} + N_{2(g)}$$

$$\Delta_R H = +\ 45.9\ kJ/mol_{NH3} \qquad (1)$$

This endothermic reaction requires energy to break the chemical bond within ammonia and temperatures above 180 °C to be thermodynamically feasible [14]. The reaction is further favored at high temperatures and low pressures. Ammonia decomposition can be accomplished via thermal cracking, catalytic cracking or steam cracking [15].

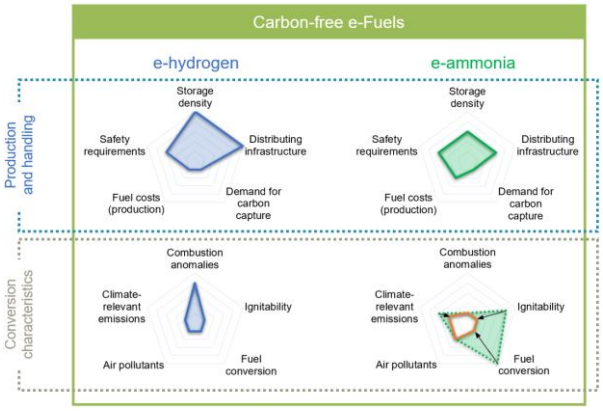

Figure 1: Assessment of carbon-free e-fuels with regard to production, handling, and conversion based on physical properties

Overall, hydrogen offers advantages in production, while ammonia is easier to store, transport and handle (Figure 1).

2.2 Ammonia and hydrogen in large engine applications

For a fuel to be deemed appropriate for engine use, it is essential that the initiation and progression of combustion can be reliably managed, and that the heat release rate is sufficient to achieve high conversion efficiencies. The low minimum ignition energy and wide flammability limits of hydrogen increase the risk of combustion anomalies. These anomalies can be classified by location, timing, and effect on the cylinder charge or intake manifold (Figure 2). Normal combustion shows expected cylinder pressure rise and heat release after ignition timing. In pre-ignition cycles, heat release starts during the compression stroke before ignition timing, causing higher peak cylinder pressures. Backfire happens earlier when intake valves are open, increasing intake manifold pressure and risking serious damage to the intake system.

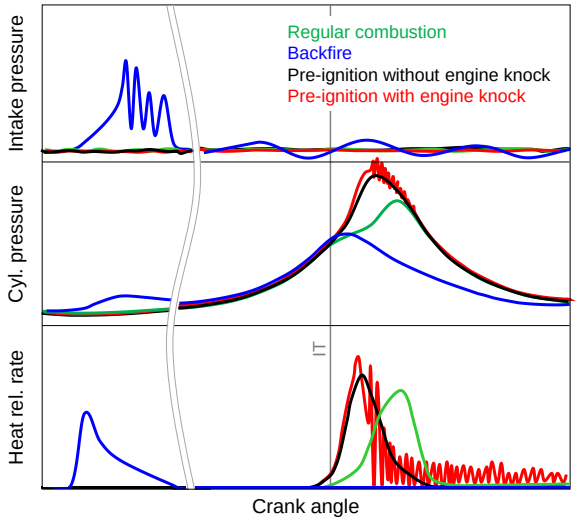

Figure 2: Cylinder and intake manifold pressure traces and heat release rate curves for characteristic regular and irregular combustion cycles

The ignition and combustion properties of ammonia seem less than ideal compared to state-of-the-art fuels. Especially the low laminar flame speed and the high minimum ignition energy were considered to be detrimental for use in an internal combustion engine. To overcome the challenges posed by the ammonia properties, admixing of a more reactive fuel, such as hydrogen or diesel fuel, was proposed [16]. In fundamental experiments [17] and engine applications, the operating conditions, particularly the turbulence levels, varied considerably, leading to a wide range of required proportions of high reactivity fuel. In recent years, ammonia cracker developments have been specifically tailored for engine-based applications, meaning only small amounts of ammonia need to be decomposed into hydrogen to act as an ignition and combustion promoter, with minimal to no purity requirements for the produced hydrogen [18], [19].

Exhaust gas emission profiles vary significantly between fuels and can be classified into pollutant emissions, which may or may not be regulated by local emission laws, and climate-relevant emissions. In hydrocarbon-fueled engines, nitric oxide (NO) is formed through the oxidation of dissociated atmospheric nitrogen at high temperatures in the presence of oxygen, a process well predicted by the Zeldovich chemical kinetic mechanism [20]. In ammonia combustion, NO formation from the oxidation of fuel-bound nitrogen also plays a role. Westlye et al. [21] found that this reaction path dominates under fuel-lean conditions, causing NO emissions to peak at an excess air ratio (EAR) of 1.35 in a spark-ignition engine. Yousefi et al. [22] observed that NO emissions were lower in diesel-ammonia dual fuel combustion compared to

pure diesel, and that later in the combustion process, NO is reduced by the thermal $DeNO_X$ process, with ammonia (NH_3) acting as a $DeNO_X$ agent [23]. The emission of nitrous oxide (N_2O), typically a result of exhaust gas aftertreatment in hydrocarbon-fueled engines [24], becomes more significant in ammonia-fueled engines due to its high global warming potential. According to the IPCC, N_2O has a GWP 273 times that of CO_2 over a 100-year timescale [25].

2.3 Ammonia and hydrogen combustion concepts

Various combustion concepts are being explored for ammonia and hydrogen-fueled engines, including both compression ignition (CI) and spark ignition (SI) approaches. The ammonia concepts that have reached the experimental validation stage primarily use a high-reactivity fuel as an ignition enhancer for at least part of the engine's operating range. Typically, diesel fuel is used as the ignition enhancer in maritime applications, while hydrogen or cracked ammonia are used for land-based applications. A schematic overview of the combustion concepts currently being experimentally validated at LEC GmbH is shown in Figure 3. Compression ignition of an ammonia-air mixture is feasible in principle but to achieve the high auto-ignition temperature of ammonia compression ratios (CR) beyond 30:1 or pre-heating of the intake air would be required, which is unreasonable for high-power applications where brake mean effective pressures of at least 20 bar have to be achieved. Therefore, only ammonia-diesel dual fuel combustion is considered for the compression ignition concepts. Multiple ammonia admission concepts are being explored. Gaseous low-pressure ammonia admission can be achieved either by centrally mixing ammonia with air upstream of the turbocharger (NH_3-CGM) or by introducing ammonia via port fuel injection (PFI). Diesel is directly injected into the combustion chamber at the end of the compression stroke to initiate combustion, which relies on flame propagation within the ammonia-air mixture. This concept also allows for pure diesel operation, making it a viable retrofit solution. The combustion process of liquid high-pressure ammonia injection (NH_3-HPDI) is similar to traditional diesel combustion, where fuel-air mixing controls the combustion. This concept uses either two fuel injectors in the combustion chamber or a two-needle injector, requiring significant modifications to the cylinder head. The design of ammonia high-pressure injectors must consider ammonia's corrosiveness, poor lubricity, and the risk of cavitation, as well as the need for high flow rates due to ammonia's lower heating value compared to diesel.

Spark ignition concepts range from direct ignition systems with a centrally mounted spark plug in the main combustion chamber (NH_3-CGM Open Chamber) to pre-chamber (PC) ignition systems with various scavenging methods (NH_3-CGM PC). The pre-chamber concept allows for mixture stratification, with a fuel-rich mixture in the pre-chamber or additional hydrogen injected directly into the pre-chamber to improve ignition conditions at the spark plug location. Directly adding hydrogen to the pre-chamber, rather than the intake mixture, could reduce the overall hydrogen fuel fraction required, leading to a smaller ammonia cracker unit and improved total system efficiency. These engine concepts rely on external mixture formation of gaseous ammonia and air, either upstream of the turbocharger or via port fuel injection. For all CI and SI combustion concepts, the high knock resistance of ammonia with a research octane number above 130 allows the use of high compression ratios.

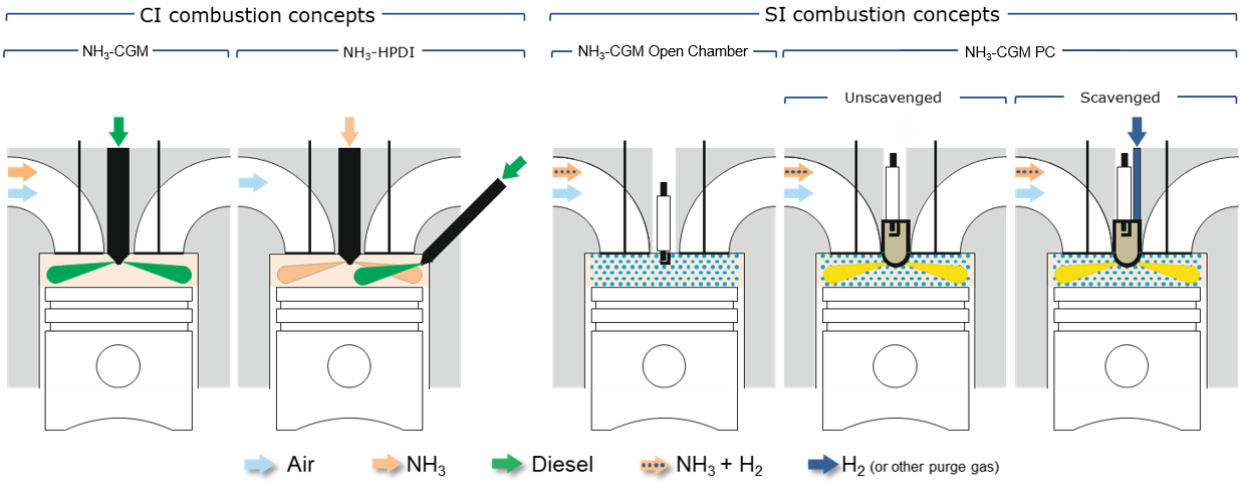

Figure 3: Ammonia combustion concepts for compression ignition engines (left) and spark ignition engines (right)

Hydrogen combustion concepts show a similar variability as ammonia combustion concepts. For CI concepts, hydrogen also benefits from the addition of a high reactivity fuel due to its high auto-ignition temperature. In this study only SI hydrogen combustion is considered and assessed based on previously published data [26].

3 EXPERIMENTAL TEST SET-UP AND PROCEDURES

The experimental assessment of different ammonia and hydrogen combustion concepts was performed on various high-speed and medium-speed single cylinder research engines (SCE) with displacement volumes between 3 and 15 liters (Figure 4). As the research engine has no turbocharger, the charge air pressure in the intake manifold was generated by an external screw-type compressor and the back pressure in the exhaust pipe was controlled by a flap. To ensure defined and accurately reproducible engine operating conditions, extensive external conditioning systems for coolant, lubricating oil, charge air and ambient air were used on the test bed.

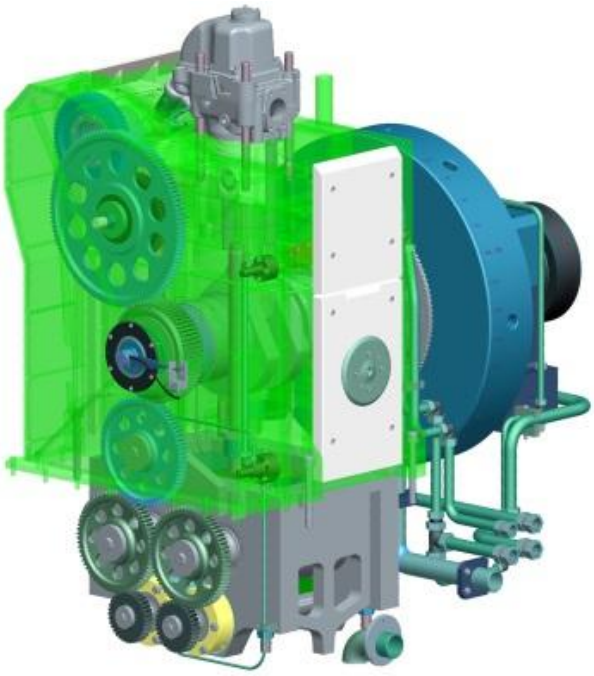

Figure 4: Singe-cylinder research engine

The ammonia supply for the engine test cell is provided by a mobile container that can store up to 2000 kg of ammonia in liquid form. The ammonia is either delivered to the test cell in liquid form or a temperature-controlled vaporizer unit provides a constant supply of gaseous ammonia to the engine test cell. The fuel supply infrastructure provides the flexibility to add hydrogen in adjustable quantities to the ammonia upstream of the fuel-air mixer. A temperature-controlled catalytic exhaust aftertreatment system ensures that no elevated levels of pollutants are released into the environment. Advanced ammonia and NO_X sensors are installed for pre-catalyst and post-catalyst monitoring, and detailed exhaust gas specification is provided by FTIR measurements.

Hydrogen was stored in gaseous form in pressurized tanks and supplied to a port fuel injection valve in the cylinder head intake duct via a gas control system that enabled accurate control of a target differential pressure compared to the intake manifold pressure. The fuel mass admitted to the engine was adjusted via the energizing time of the PFI valve.

Three different ammonia combustion concepts were investigated:

NH_3-CGM PC SI: Gaseous ammonia, hydrogen and charge air were homogeneously mixed before being carried into the cylinder during the intake stroke. The pre-chamber was centrally located in the cylinder head.

NH_3-CGM CI: For this dual-fuel concept, ammonia in gaseous form and air were homogeneously mixed upstream of the cylinder. The diesel pilot injector was located centrally in the cylinder head.

NH_3-HPDI CI: For the HPDI concept, the cylinder head was modified to accommodate two injectors. The ammonia common rail injector [27] was located centrally in the combustion chamber, replacing a conventional diesel injector, and a second injector was integrated into the cylinder head in a laterally inclined position to provide the diesel pilot injection. The positioning and orientation of the diesel injector nozzle in the combustion chamber required a special orifice configuration. An illustration of the fuel spray interaction of the diesel spray and the ammonia spray is shown in Figure 5.

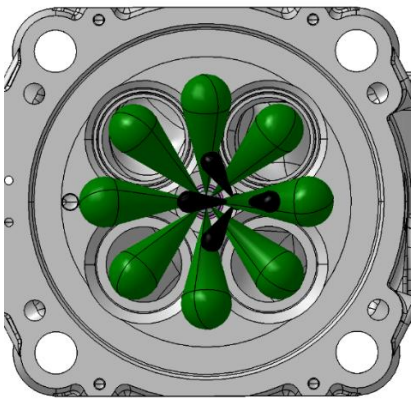

Figure 5: Illustration of diesel pilot (black) and ammonia (green) fuel jet interaction

The dual fuel combustion concept with separate injectors for diesel and ammonia allows an independent adjustment of the dwell duration between the injection of the two fuels. Figure 6 illustrates the definition of the dwell which describes the crank angle duration from the start of the diesel injector current signal to the start of the ammonia injector current signal. Due to the hydraulic delay the injection starts later than the injector current signal which is indicated by the rail pressure drop (shown for ammonia in Figure 6). The hydraulic delay of the diesel injector amounts to only a few degrees crank angle (°CA) while the ammonia injector hydraulic delay is longer (around 10 °CA) and varies with the rail pressure. Since the detection of the start of injection is subject to a higher uncertainty than the injector current signal, the dwell timing was calculated based on the injector current signals throughout the article. The ammonia injection pressure could be varied between 600 bar and 1300 bar. Diesel injection pressures up to 1200 bar were used.

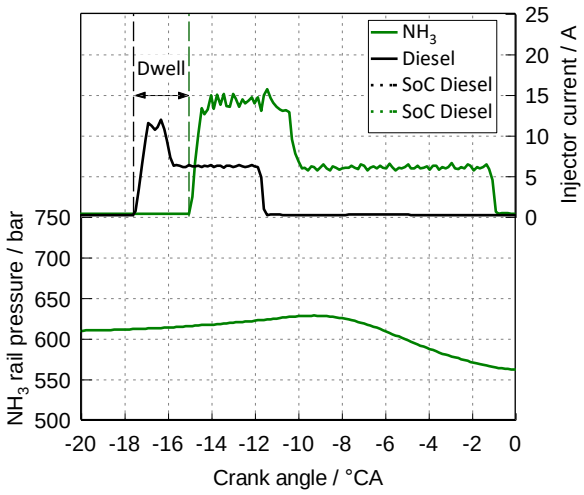

Figure 6: Definition of dwell, injector current signals and ammonia rail pressure trace

The ammonia combustion experiments in the following section each have been performed at a fixed brake mean effective pressure and fixed engine speed (although there is a difference in the operating condition between the different combustion concepts). The boost pressure was adjusted to achieve the target EAR at each operating condition. The EAR is taking the mass of NH_3 and the mass of diesel (Equation 2) or the mass of H_2 (Equation 3) into account, depending on the investigated combustion concept.

$$EAR = \frac{m_{\mathrm{Air}}}{m_{\mathrm{NH3}} \cdot AFR_{\mathrm{NH3}} + m_{\mathrm{Diesel}} \cdot AFR_{\mathrm{Diesel}}} \quad (2)$$

$$EAR = \frac{m_{\mathrm{Air}}}{m_{\mathrm{NH3}} \cdot AFR_{NH3} + m_{\mathrm{H2}} \cdot AFR_{\mathrm{H2}}} \quad (3)$$

The diesel ($\varphi_{\mathrm{Diesel}}$) and hydrogen shares ($\varphi_{\mathrm{H2}}$) in the fuel mixtures are calculated as energetic fractions based on their heating values.

The investigation of different ammonia combustion concepts focused on high load operation and the achievable operating windows in terms of EAR and ammonia substitution rates. In addition, the key influencing parameters on the main exhaust gas species nitrogen oxides, nitrous oxide and unburnt ammonia were evaluated. Other performance parameters such as efficiency, charge pressure demand or peak cylinder pressure are investigated in the following chapter based on 1D simulations with boundary conditions from the experimental investigations.

The investigation of the NH_3-CGM CI concept was conducted at full load operating conditions with EAR variations at different diesel energy fractions. Starting from a typical diesel operating condition with an EAR of about 1.9, ammonia was added to the intake charge air while the diesel injection duration was reduced. All other operating parameters such as intake charge temperature and humidity and combustion phasing were kept fixed. The investigation of the NH_3-HPDI concept did not allow operation with 100 % diesel fuel because only a diesel pilot injector was installed. Therefore, the diesel energy fractions were only varied between 5 and 20 %.

For the NH_3-CGM PC SI concept EAR variations were performed for energetic hydrogen fractions up to 8 % at full load. Higher hydrogen fractions are feasible, but due to the fact that ammonia cracking affects system efficiency and operating costs, the focus was on using the smallest amounts of hydrogen possible.

Two hydrogen combustion concepts were investigated with a pre-chamber located centrally in the cylinder head:

H_2-PFI PC SI: Gaseous hydrogen was admitted into the intake port during the intake stroke via a port fuel injection valve with hydrogen pressures up to 8 bar.

H_2-DI PC SI: Gaseous hydrogen with injection pressures up to 30 bar was injected into the cylinder after the intake valves were closed.

No second fuel was added for the hydrogen combustion concept investigations.

4 EXPERIMENTAL RESULTS

4.1 NH_3-CGM CI combustion concept

The full load operating map with the NH_3-CGM CI concept is illustrated in Figure 7 and shows that the feasible EAR range shifted with the diesel energetic fraction. Over a wide EAR range the diesel fraction could be reduced down to approximately 2 %. For high diesel energetic fractions, the high EAR of pure diesel operation is achievable but the operation with low EAR was limited to 1.4 and 1.3 for 80 % and 60 %, respectively, due to increasing emissions of carbon monoxide. The opposite trend was observed for low diesel energetic fractions where the lowest EAR of 1.2 was achievable but high EAR operation was limited due deteriorating combustion stability and increasing NH_3 emissions.

The brake specific exhaust gas emissions nitrogen oxides, nitrous oxide, ammonia are depicted in color coded contour plots in Figure 7. Emissions of unburned NH_3 stem from various sources. Apart from incomplete combustion, NH_3 emissions from crevices have to be taken into account. Due to the ammonia admission in the intake manifold also the NH_3 emission from scavenging losses during the valve overlap need to be considered. Experimentally these different sources cannot be differentiated easily. Two trends can be observed. For a given diesel energetic fraction the NH_3 emissions are reduced with lower EAR. This can be explained by the higher flame speed and therefore the faster flame propagation in the ammonia-air mixture, the increased gas temperature and the lower in-cylinder pressure propagating flame cannot be well sustained. With the lower diesel fraction there is more gas in the combustion chamber that is not completely consumed by the diesel jets and also cannot be burned via flame propagation. Additionally, the higher ammonia fraction leads to more ammonia mass in the crevices that might escape combustion.

The NO_X emissions show a strong increase with higher ammonia shares. In addition, there is a trend for higher NO_X emission with increasing EAR that is occurring for higher diesel fractions.

The dominating influence of the EAR on the N2O emission that was described in the literature can be seen clearly in Figure 7. The lowest N2O emissions are achieved with EAR=1.2. The diesel energetic fraction also seems to have an impact, particularly at high EAR.

4.2 NH_3-HPDI CI combustion concept

The goal of the experimental investigations with ammonia direct injection (DI) was to assess the impact of operating parameters such as EAR and combustion phasing. The energetic diesel fraction was maintained at 10 % and the dwell duration was fixed at 2.5 °CA. The injection timing had to be advanced towards lower EAR in order to maintain the desired combustion phasing which is mainly driven by a longer ignition delay time and the early part of the combustion process. At an EAR of 1.2 also the later part of the combustion shows a retarded timing. The process for the lower EAR is not just characterized by a delayed heat release but also by a less complete combustion as can be seen in the emissions of unburned

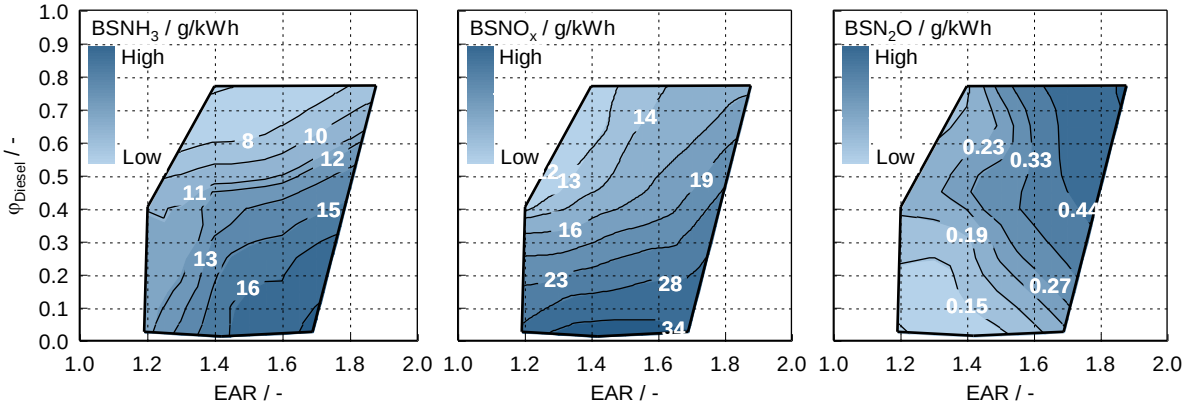

Figure 7: NH_3-CGM CI operating windows and NH_3, NO_X and N_2O emissions

that reduces the amount of unburned fuel in the crevices at the end of the combustion. The impact of the diesel energetic fraction is most clearly seen at high EAR where the NH_3 emission increases with lower diesel fraction. In this range the EAR in the ammonia-air mixture is very high such that a ammonia that are displayed in Figure 8. While the measured NH_3 concentrations in the exhaust gas are nearly constant between EAR = 1.4 and 1.8 there is a significant increase for EAR = 1.2. The opposite is observed for the emissions of nitrogen oxides that are lower for EAR = 1.2 than for the

higher EAR. While the retarded and less complete combustion might contribute to this behavior, oxygen availability is likely the dominating factor. This is in line with the trends reported in the literature for (partially) premixed combustion where maximum nitrogen oxide emissions were found to occur at approximately EAR = 1.35 [21]. Taking the changing efficiency and exhaust gas mass flow rates for different EAR into account the NO_X emission intensity for EAR = 1.2 was found to be approximately 40 % of that for the higher EAR.

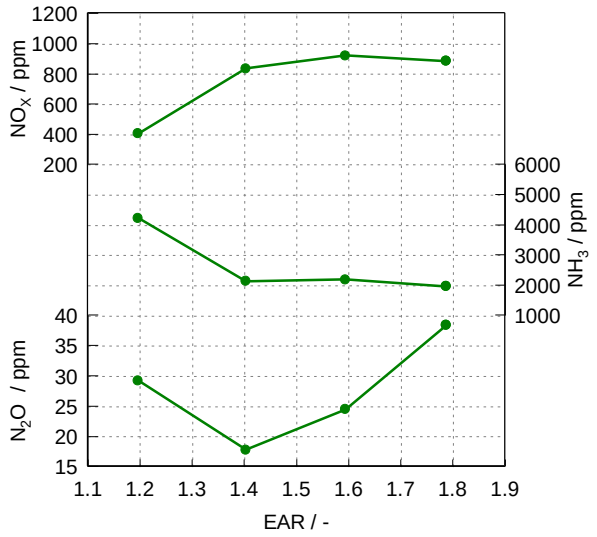

Figure 8: NH_3-HPDI CI: NH_3, NO_X and N_2O emissions for an EAR variation

The nitrous oxide emissions are on a relatively low level below 50 ppm. They are decreasing with decreasing EAR from 1.8 – to 1.4. For EAR = 1.2 an unexpected increase of the nitrous oxide emissions was observed. Since this increase is occurring in conjunction with a strong increase of the ammonia concentration it is possible that the nitrous oxide (or at least some share) is not formed during the main combustion phase but rather in the expansion and exhaust stroke when the unburned ammonia is reacting with nitrogen oxides at low temperature in a reaction known as selective non-catalytic reduction. The results show that the EAR for ammonia-diesel dual fuel operation can be varied in a wide range and that an EAR similar to values for typical diesel engines is feasible.

For a comparison of NH_3-HPDI and diesel operation a combustion phasing variation was performed for an EAR = 1.8. The diesel operation was investigated with a diesel injector located in a central position in the cylinder head, in lieu of the ammonia injector. The cyclic variability of the ammonia operation was higher than for diesel operation throughout the combustion phasing variation (Figure 9). Up to CA50 = 12 °CA after top dead center (aTDC) the coefficient of variation of the indicated mean effective pressure (COV_{IMEP}) could be maintained below 1.5 %. For the latest combustion phasing of CA50 = 16 °CA aTDC the cyclic variability increased significantly which might be explained by a weaker combustion initiation.

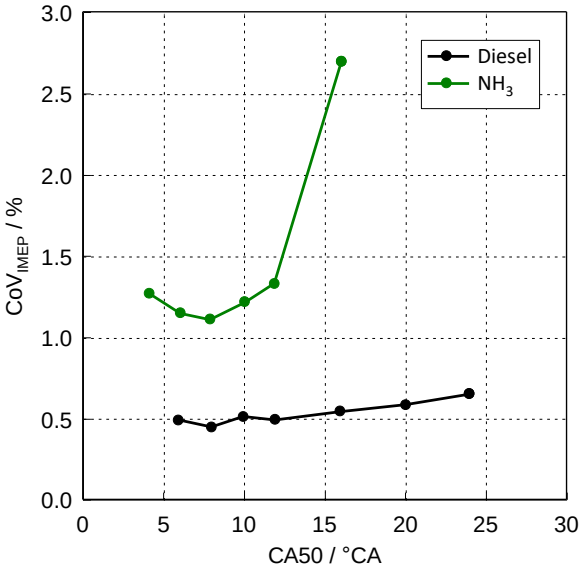

Figure 9: NH_3-HPDI CI: Comparison of cyclic variability for ammonia and diesel operation for a combustion phasing variation

A comparison of the NO_X emissions (Figure 10) showed that, rather unexpectedly, for the same combustion phasing (and same EAR) the emissions for ammonia operation are lower than those from the diesel operation.

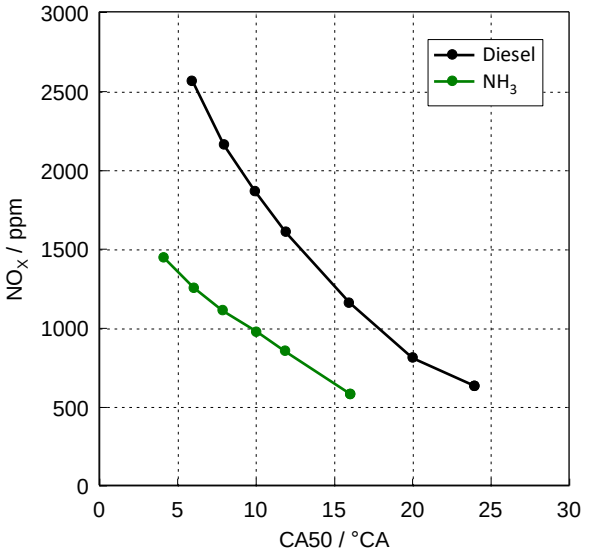

Figure 10: NH_3-HPDI CI: Comparison of NO_X emissions for ammonia and diesel operation for a combustion phasing variation

This behavior is probably caused by a combination of two effects. On the one hand, the heat of vaporization of ammonia is significantly higher than that of diesel. On the other hand, the adiabatic flame temperature of ammonia is lower than that of diesel (for stoichiometric blends), which affects the overall in-cylinder temperature. This effect on the in-cylinder temperature strongly influences the thermal NO_X formation, which is typically the dominant fraction in hydrocarbon fuels. For ammonia combustion, this temperature effect is combined with NO_X formation from fuel-bound nitrogen. In this particular case the ammonia operation showed a more favorable fuel consumption – NO_X emission trade-off than the diesel operation.

4.3 NH_3-CGM PC SI combustion concept

The investigated operating window for the NH_3-CGM PC SI concept is shown in comparison to the NH_3-CGM CI concept in Figure 11. Compared to typical hydrogen or natural gas operation the EAR was reduced to (partially) compensate the lower combustion velocity of ammonia. The achievable operating range is limited by increased cyclic variability with high EAR and high NH_3 emissions with low EAR and depends on the fraction of hydrogen addition. Operation without any hydrogen admixture is feasible but only in a narrow EAR range of 1.2. – 1.3. Adding a small amount of hydrogen, even as low as 4 %, significantly widens the achievable EAR range because the higher reactivity of hydrogen is compensating for the reactivity decrease with higher dilution. The brake specific exhaust gas emissions nitrogen oxides, nitrous oxide, ammonia and the carbon dioxide equivalent are depicted in color coded contour plots. The origin of the emission of unburned NH_3 is assumed to be similar to the NH_3-CGM CI combustion concept, although due to the reduced valve overlap a lower contribution of scavenging losses can be expected. On the other hand, there is additional crevice volume associated with the pre-chamber. The hydrogen fraction is strongly impacting the NH_3 emissions where increasing hydrogen fractions lead to lower NH_3 emissions due to the higher reactivity and reduced flame quenching. A reduced EAR results in an earlier end of the combustion process and therefore a higher pressure and more mass trapped in the crevice volumes.

The NO_X emissions are dominated by the EAR and show only a small impact of the hydrogen fraction due to increased burning velocity. The NO_X concentrations in the exhaust gas reach their maximum values for EAR between 1.25 and 1.3, slightly below the values that were reported in the literature for pure ammonia combustion.

The EAR also has a dominating influence on the N_2O emissions. Similar to the NH_3-CGM CI concept the lowest N_2O emissions are achieved with the lower EAR and are overall in a similar range.

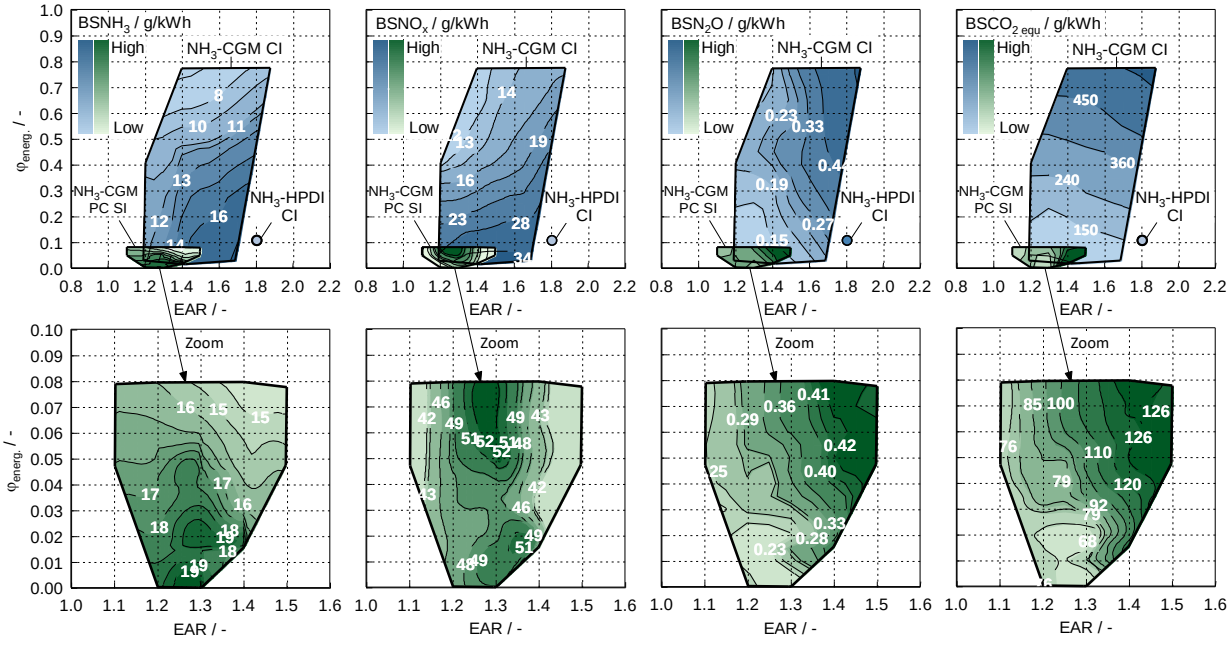

Figure 11: Comparison of NH_3, NO_X, N_2O and CO_2-equivalent emissions in NH_3-CGM PC SI and NH_3-CGM CI operation

In order to assess the global warming potential (GWP) of the exhaust gas components the CO_2 equivalent emissions are calculated based on CO_2 and N_2O emissions for both ammonia CGM combustion concepts. For the CI concept the lowest CO_2 equivalent emissions can be achieved with low diesel energetic fractions and low EAR. At this condition a reduction in the GWP of approximately 75 % (compared to diesel operation with about 600 g/kWh CO_2 emissions) can be achieved. The CO_2 equivalent emissions are drastically lower for the NH_3-CGM PC SI concept due to the absence of CO_2 emissions, reaching about 90 % lower values than diesel operation. Due to the high global warming potential of nitrous oxide a further reduction via exhaust gas aftertreatment is still required.

4.4 Hydrogen PFI and DI combustion concepts

Hydrogen port fuel injection concepts with high dilution ratios (> 2.0) can achieve high power densities without excessive risk of combustion anomalies. The high dilution with air or exhaust gas or water injection also ensures low knock intensity and low NO_X emission levels. One of the major drawbacks of high dilution levels is the high boost pressure demand. The achievable compressor pressure ratio and turbocharger efficiency were found to set clear limits to the potentially feasible excess air ratio and power density of the engine. Hydrogen direct injection, when taking place after intake valve closing, prevents the occurrence of backfiring into the intake manifold, has the potential for higher volumetric efficiency and is regarded as a key technology component for increasing power density. The investigation of the different direct injection strategies showed that there is a trade-off between the benefits of higher volumetry efficiency and the avoidance of backfiring on the one hand and the negative impact on knocking and emission formation on the other hand.

In order to assess the performance of the DI concept in comparison to a PFI concept different operating points have been plotted on a NO_X emission vs. dilution map (Figure 12). The colors in the plots represent the boost pressure, COV_{IMEP} and knock intensity, respectively. Even though the exact operating conditions cannot be matched between port fuel injection and direct injection points, it can be seen that with port fuel injection significantly lower NO_X emissions could be achieved with the same dilution rate. The boost pressure demand for a given dilution rate is lower for the direct injection due the hydrogen admission after the intake valves have been closed but the COV_{IMEP} and the knock intensity are higher than for the port fuel injection.

4.5 Selection of configurations and operating conditions

The experimental assessment of ammonia and hydrogen combustion concepts allowed the selection of geometry and operating boundary conditions for a comparative performance assessment of these fuels.

- The high knock resistance of ammonia enables “diesel-like” CR for CI concepts and efficiency optimum combustion phasing
- NH_3 concepts with premixed combustion favor lower EAR, whereas an HPDI concept enables “diesel-like” EAR
- NH_3 concepts with premixed combustion require less than 5 % of high reactivity fuel at full load operation
- H_2 concepts require high dilution rate and for premixed combustion concepts moderate CR to mitigate knocking combustion

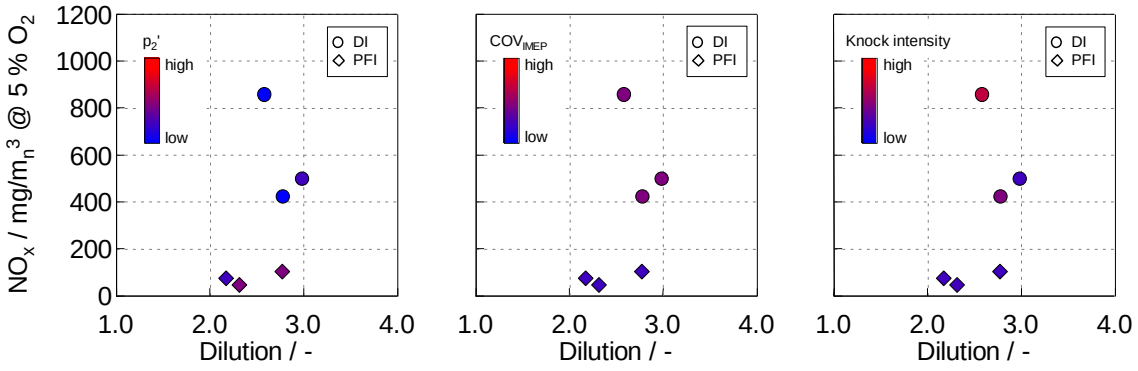

Figure 12: Comparison of selected performance parameters for PFI and DI hydrogen combustion concepts

5 COMPARATIVE ASSESSMENT OF AMMONIA AND HYDROGEN COMBUSTION

In order to enable a comparison of the different combustion concepts presented in the previous sections without any biasing impact of different engine sizes and engine speed as well as testbed-related uncertainties, 1D engine performance simulations were carried out with the software tool GT-Power from Gamma Technologies. Methodology, simulation results and their discussion are presented in the following section.

5.1 Methodology

For the simulation-based investigation a generic V16 diesel engine model with a displacement of 76.3 liters was modified to account for the needs of the different combustion concepts.

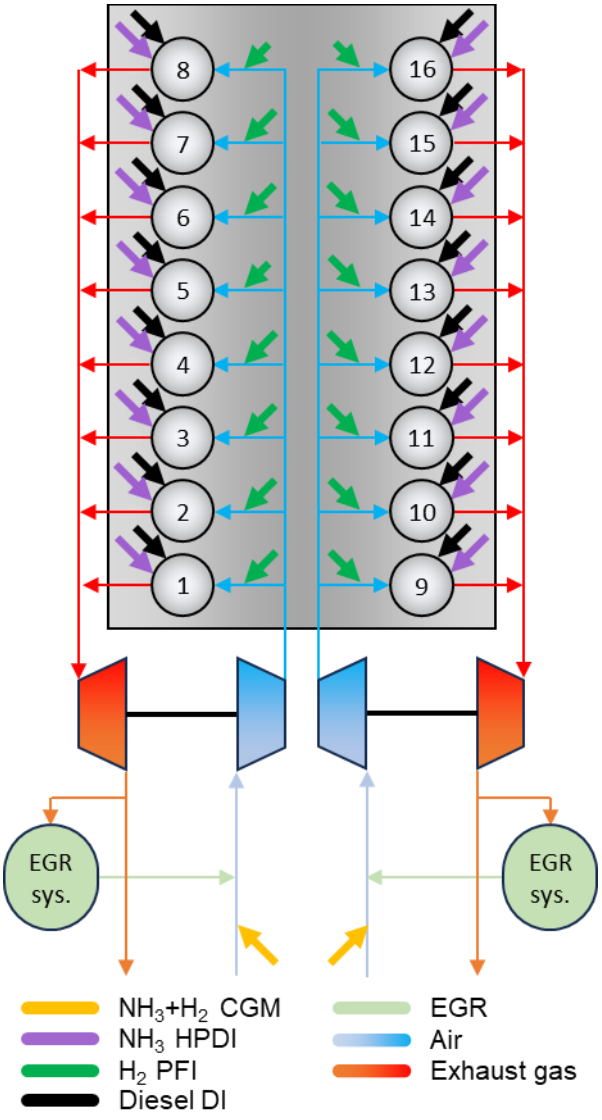

Figure 13: Engine layout of the GT-Power model with fuel, EGR, air and exhaust gas paths

The modifications included: fuel injectors for central gas mixing (CGM), PFI and DI, a single-stage turbocharger for each cylinder bank with prescribed efficiency as well as a low-pressure exhaust gas recirculation (EGR) system were implemented. While the EAR was controlled via waste gates incorporated in both turbines, the engine power was adjusted via the injected fuel mass and the EGR rate was modified via a flap in the exhaust gas system. The heat transfer model including the calculation of the heat transfer coefficient was not modified for any particular fuel or combustion concept. A simplified layout of the combustion engine is presented in Figure 13.

Boundary conditions for both hardware and operating parameters, such as CR or fuel injection timing, were derived from the SCE experimental results presented in the previous chapter, except for engine brake power and engine speed, which were set to 2000 kW and 1500 min^{-1}, respectively. Combustion phasing was set to CA50 = 8 °CA aTDC and combustion progress was imposed by specifying heat release rates, which were generated based on cylinder pressure traces using the software tool CORA from LEC GmbH. Pre-chamber heat release was omitted in this study to avoid unnecessary complexity. Fuel fractions of a high-reactivity fuel for the ammonia engine configurations were set to 10 % for the HPDI configuration and 2.7 or 2.0 % for CGM CI and CGM PC SI, respectively. Table 2 summarizes engine hardware parameters as well as operating conditions of the selected engine configurations for the simulation-based assessment. Three hydrogen engine configurations with port fuel injection and pre-chamber ignition were selected. They are differentiated by different dilution levels and the selected diluent, i.e., excess air or EGR. The ammonia engine configurations are reflecting those investigated experimentally, i.e., NH_3-CGM CI, NH_3-HPDI CI and NH_3-CGM PC SI.

5.2 Simulation-based assessment

The assessment of the simulation results in this section is focused on engine performance parameters as well as system parameters, such as indicated engine efficiency, compressor pressure ratio or post-turbine exhaust gas temperature, the latter being an important parameter for the exhaust aftertreatment.

Engine performance parameters

In Figure 14 simulation results for key performance parameters are presented for all six selected engine configurations. The compressor pressure ratios of the three hydrogen configurations show

Table 2: Engine hardware parameters and operating parameters of the selected engine configurations

Parameter \ Configuration	H_2 PFI	H_2 PFI EGR v1	H_2 PFI EGR v2	NH_3-HPDI CI	NH_3-CGM CI	NH_3-CGM PC SI
Engine brake power / kW				2000		
Engine speed / min^{-1}				1500		
CA50 / °CA				8.0		
EAR / -	2.75	1.3	1.0	1.8	1.4	1.25
φ_{EGR} / $\%_{wt.}$	0	48	56	0	0	0
Dilution[1] / -	2.75	2.49	2.36	1.8	1.4	1.25
φ_{Diesel} / $\%_{energ.}$	0	0	0	10.0	2.7	0
φ_{H2} / $\%_{energ.}$	100	100	100	0	0	2.0
CR / -	11.5:1	11.5:1	11.5:1	17:1	17:1	13.5:1
Valve timing / -				Miller		
Fuel admission / -	PFI	PFI	PFI	DI	CGM (NH_3) DI (Diesel)	CGM
Ignition concept / -	Pre-chamber spark ignition			Diesel pilot	Diesel pilot	Pre-chamber spark ignition

some differences due to different dilution levels and are significantly higher compared to those of the NH_3 engine configurations, which can be attributed to the higher stoichiometric air-fuel ratio of H_2 compared to NH_3, the higher dilution as well as the displacement of air by H_2 due to the PFI concept being used. With a compressor pressure ratio of around five, single-stage turbocharging might reach its limits for H_2 operation with high dilution levels. The higher intake and exhaust gas pressure levels of the H_2 engine configurations result in different gas dynamics and are reflected in higher pumping mean effective pressures (PMEP).

The peak cylinder pressure shows a relatively wide spread of 50 bar with no clear distinction between the H_2 and NH_3 configurations. The three H_2 configurations show a spread in peak cylinder pressure of about 15 bar, which correlates with the level of dilution. The H_2 configurations ranged somewhere between the lowest and highest NH_3 configurations. Several effects are superimposed: the charge air pressure and thus the starting pressure for compression, the compression ratio, the shape of the heat release rate - especially in the late part of the combustion - and the physical gas properties, i.e., the specific heat ratio. The latter leads to the counterintuitive observation that if NH_3 is present in the combustion chamber during compression, the cylinder pressure at the end of compression is significantly lower than would be expected from the compression ratio alone.

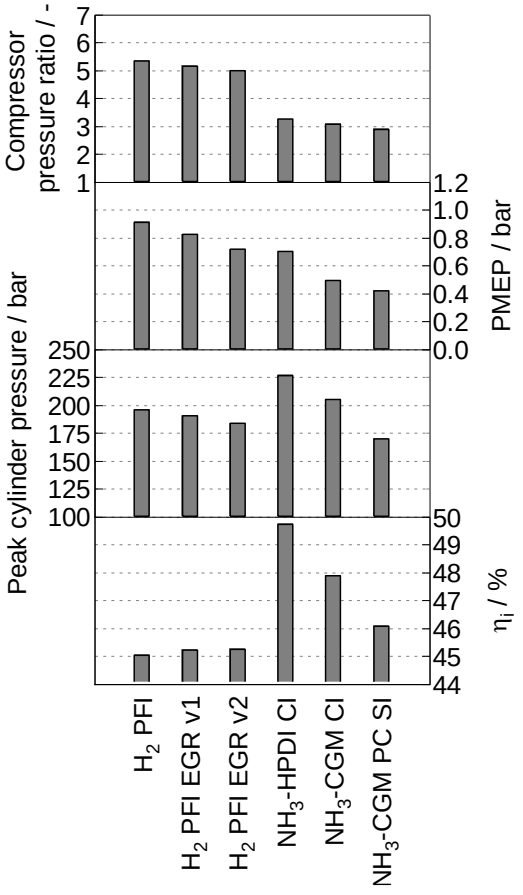

Figure 14: Key performance parameters of the selected engine configurations

[1] Dilution is defined as the sum of air and EGR mass flow rates divided by the stoichiometric air demand and thus equal to the EAR for cases without EGR.

The higher indicated efficiencies (η_i) of the NH_3 configurations can be attributed to the higher CR's used compared to the H_2 configurations, the aforementioned lower pumping losses as well as lower compression work due to more favorable fluid properties. A more detailed look on the efficiencies will be provided later.

As illustrated in Figure 15, a clear trend does not emerge when comparing the hydrogen and ammonia cases in terms of the exhaust gas temperature upstream of the turbine (T_3), as multiple factors influence this parameter, including compression (or expansion) ratio, the combustion process, and dilution. In the case of hydrogen, it is primarily the dilution that leads to fluctuations in T_3. However, a distinct trend is observed for the post-turbine temperature (T_4), with ammonia cases consistently exhibiting higher values. This is due to the lower power demands of the compressor, resulting from lower pressure ratios, which cause smaller temperature drops (ΔT_{34}) across the turbine, ultimately leading to higher post-turbine temperatures. Additionally, the increased wastegate mass flow rates in the ammonia cases further elevate T_4.

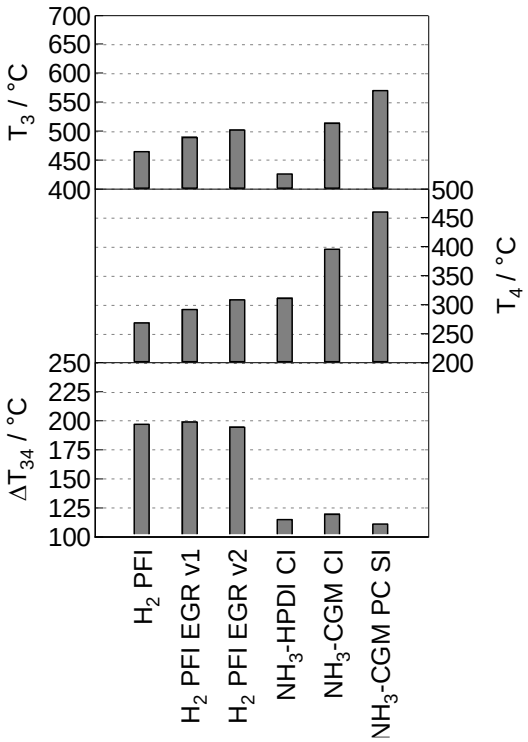

Figure 15: Pre- and post-turbine exhaust gas temperature and temperature drop across the turbine of the selected engine configurations

The simulation results also provide valuable insight into potential improvements. For example, the relatively low peak firing pressures observed in the hydrogen and premixed ammonia cases suggest the possibility of implementing higher compression ratios, which would improve engine efficiency and reduce compressor pressure ratios. Further reductions in compressor pressure ratios could be achieved by implementing filling optimized valve lift profiles. However, it is important to note that, particularly for hydrogen operation, higher CRs could also increase the risk of abnormal combustion phenomena such as knock - an effect that will need to be evaluated either through experimental investigations or more sophisticated simulation approaches such as 3D-CFD simulations or detailed chemical kinetics simulations.

Efficiency loss analysis

An efficiency loss analysis was performed with GT-Power to determine certain influences on the efficiency and to identify further potential for improvement. This analysis quantifies several sources of cylinder efficiency losses from a theoretical maximum. In the present work, this maximum is defined as the ideal cycle efficiency combined with the efficiency losses due to real fluid properties, i.e., temperature and pressure dependent thermodynamic properties, and real cylinder charge composition. This value is obtained for the high-pressure phase of the engine cycle based on several assumptions, such as instantaneous combustion at top dead center, no heat transfer and loss-free gas exchange. In the following, this value is referred to as the efficiency of the ideal engine with real charge (η_{ie}). Subsequently, losses due to incomplete combustion ($\Delta\eta_{ic}$), combustion duration and phasing, collectively referred to as the loss due to real combustion ($\Delta\eta_{rc}$), heat transfer ($\Delta\eta_{ht}$), as well as expansion, compression, and gas exchange, summarized as the gas exchange loss ($\Delta\eta_{ge}$), are subtracted. This procedure results in the indicated efficiency of the respective cylinder for which the loss analysis was performed. The outcome of the loss analysis is presented in Figure 16.

The efficiency of the ideal engine with real charge of the H_2 configurations is already lower than the one of the NH_3 configurations, mainly because of differences in the CR's used. While the premixed ammonia combustion concepts suffer from comparatively high emissions of unburnt fuel resulting in relatively high losses due to incomplete combustion, these losses are basically non-existent for the H_2 configurations and at least lower for the NH_3-HPDI configuration. The losses due to real combustion are similar due to the identical combustion phasing. However, differences exist due to the varying shape of the specified heat release rates. With the exception of NH_3-CGM PC SI configuration, the heat transfer losses of the NH_3

configurations are higher due to higher pressure and temperature levels. For the NH_3-CGM PC SI configuration, the lower pressure level resulting from the comparatively low dilution compensates the higher temperature level during combustion. Consequently, this results in an overall lower Woschni-based heat transfer coefficient. The already presented trend in the PMEP can also be seen in the efficiency loss analysis, with higher gas exchange losses for the H_2 configurations. Likewise, the indicated efficiency trend of Figure 14 is also seen, albeit with small discrepancies. This is due to the fact that the previously shown values apply to the complete engine while the values in Figure 16 are only valid for a certain cylinder. This is a minor shortcoming of the chosen GT-Power simulation approach but does not invalidate the conclusions.

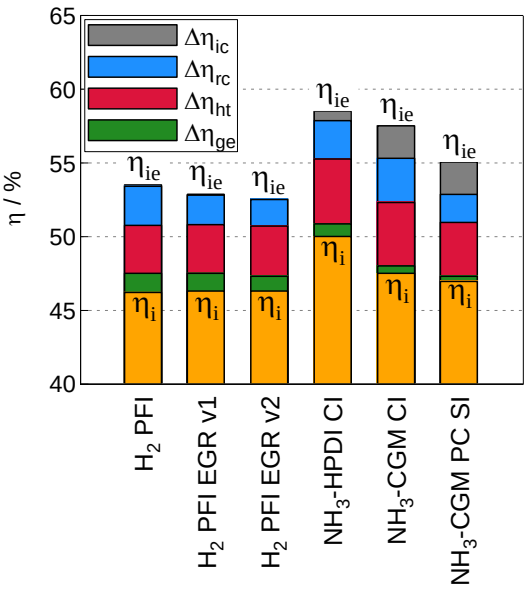

Figure 16: Efficiency loss analysis of the simulated combustion concepts

Exhaust aftertreatment

Another important factor to consider when comparing the different combustion concepts is their significantly varying NO_X emissions. In this study, a NO_X emission limit of 25 mg/m³ is assumed, and NO_X emissions are reduced through selective catalytic reduction (SCR) using an aqueous urea solution (AUS). Based on SCR reactions, measured NO_X and NH_3 emissions, and exhaust mass flow rates from the 1D simulation, the required AUS demand was determined, with the results presented in Figure 17.

As shown by the solid red bars, the hydrogen combustion concepts exhibit relatively low NO_X emissions, necessitating only small amounts of AUS. Notably, the NO_X emissions of the H2 PFI EGR v2 concept are even below the set limit, meaning no AUS is required. In contrast, the premixed ammonia combustion concepts produce significantly higher NO_X emissions than the hydrogen cases, leading to a much higher AUS demand—though this is only the case when engine-out NH_3 emissions in the exhaust are not considered. When these emissions are taken into account, the premixed ammonia concepts require comparatively little or even no AUS.

The NH_3-HPDI CI concept, however, has the highest AUS demand of all concepts, as the NH_3 in the exhaust gas is insufficient to reduce the NO_X emissions to the specified limit. For ammonia combustion concepts, an appropriate NH_3-NO_X ratio of approximately one eliminates the need for AUS altogether. Figure 17 also presents the percentage of ammonia (contained in the AUS) used for SCR relative to the ammonia used as fuel. As seen, only a small proportion of the ammonia is needed for exhaust aftertreatment.

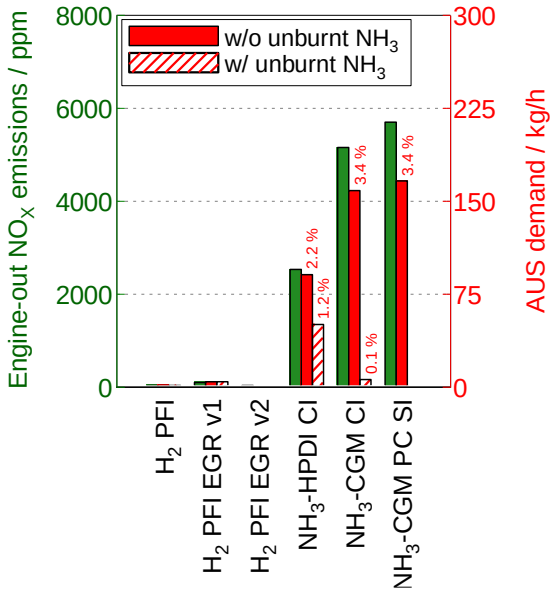

Figure 17: NO_X emissions and AUS demand of the different combustion concepts. Percentage values are the ammonia used for the SCR contained in the AUS in relation to the ammonia used as fuel

6 CONCLUSIONS AND OUTLOOK

Both ammonia and hydrogen combustion in large-bore engines have gained significant interest in recent years as potential enablers for the decarbonization of hard-to-abate energy sectors. However, when considering the complexities of fuel production, transportation, storage, and conversion within the engine, it remains uncertain whether the direct use of ammonia in the engine or the cracking

of ammonia into nitrogen and hydrogen—followed by the use of hydrogen in the engine—will be the preferred pathway for large-scale applications.

This article presents experimental investigations conducted on single-cylinder research engines and 1D performance simulations to assess the potential and challenges associated with the use of ammonia and hydrogen in large-bore engines. Different combustion concepts have been explored for both fuels, each with distinct advantages and challenges.

Ammonia has proven to be a suitable fuel, benefiting from its high knock resistance, which allows for the use of high compression ratios and consequently offers significant efficiency potential. In particular, the NH_3-HPDI CI concept stands out due to its high efficiency potential, which is further enhanced by its ability to perform well with high EAR. However, the power demand for the high-pressure fuel pump in the HPDI concept was not considered in the presented results. Moreover, since the HPDI concept already generates high peak cylinder pressures, further increases in compression ratio may be limited by the mechanical constraints of the engine. Nonetheless, NH_3 concepts with lower EAR, particularly the spark ignition concept with a lower compression ratio, present additional potential for further improvement.

For all ammonia combustion concepts, a sophisticated and highly effective exhaust aftertreatment system is required. To meet NO_X emissions targets of 25 mg/m³, SCR catalyst conversion efficiencies of around 99 % are necessary. Reducing agent demands can be minimized if the engine-out NH_3-NO_X ratio is maintained near one. Alongside NO_X reduction, effective N_2O reduction is essential due to the high GWP of this species. N_2O aftertreatment is still under development, and future research will determine the acceptable exhaust gas temperature levels for efficient treatment. Additionally, an oxidation catalyst is required to prevent NH_3 emissions.

Hydrogen engines, on the other hand, face challenges related to preignition phenomena and the need for high dilution levels, which increase the demands on the turbocharging system. The lower compression ratio used in premixed hydrogen combustion concepts results in an efficiency penalty compared to ammonia configurations. If hydrogen is produced from ammonia, an additional efficiency penalty has to be taken into account. However, the aftertreatment demands for hydrogen combustion are generally much less stringent, with fewer or no additional reduction required, depending on the specific engine design.

Further research in both fuel technologies will exploit additional efficiency potential and engine-specific optimization of the combustion system layout. Additionally, the research will focus on measures to reduce emissions of regulated and unregulated species.

7 DEFINITIONS, ACRONYMS, ABBREVIATIONS

°CA: Degree crank angle
1D: One-dimensional
3D-CFD: Three-dimensional computational fluid dynamics
aTDC: After top dead center
AUS: Aqueous urea solution
CA50: Combustion phasing
CGM: Central gas mixing
CI: Compression ignition
CO_2: Carbon dioxide
COV: Coefficient of variation
CR: Compression ratio
DI: Direct injection
ΔT_{34}: Turbine temperature drop
EAR: Excess air ratio
EGR: Exhaust gas recirculation
FTIR: Fourier transform infrared spectroscopy
GHG: Greenhouse gas
GWP: Global warming potential
H_2: Hydrogen
HPDI: High-pressure direct injection
IMO: International Maritime Organization
kW: Kilowatt
LEC: Large Engines Competence Center
NH_3: Ammonia
NO_X: Nitrogen oxides
N_2: Nitrogen
N_2O: Nitrous oxide
P: Power
PFI: Port fuel injection
PMEP: Pumping mean effective pressure
SCE: Single cylinder research engine
SCR: Selective catalytic reduction
SI: Spark ignition
T_3: Pre-turbine exhaust gas temperature
T_4: Post-turbine exhaust gas temperature
$\Delta\eta_{ge}$: Efficiency loss due to gas exchange
$\Delta\eta_{ht}$: Efficiency loss due to heat transfer
$\Delta\eta_{ic}$: Efficiency loss due to incomplete combustion
$\Delta\eta_{rc}$: Efficiency loss due to real combustion
η_{ie}: Indicated efficiency of the ideal engine
η_i: Indicated efficiency

$\varphi_{\mathrm{Diesel}}$: Energetic diesel share
φ_{EGR}: Share of the recirculated exhaust gas
φ_{H2}: Energetic hydrogen share

8 ACKNOWLEDGMENTS

The authors would like to acknowledge the financial support of the "COMET - Competence Centers for Excellent Technologies" Program of the Austrian Federal Ministry for Climate Action, Environment, Energy, Mobility, Innovation and Technology (BMK) and the Austrian Federal Ministry of Labor and Economy (BMAW) and the Provinces of Salzburg, Styria and Tyrol for the COMET Centre (K1) LEC GETS. The COMET Program is managed by the Austrian Research Promotion Agency (FFG). The authors also gratefully acknowledge funding from the Austrian Research Promotion Agency (FFG) in the project HyStore (K-Project HyTechonomy, FFG grant number 882510).

9 REFERENCES AND BIBLIOGRAPHY

[1] Copernicus Climate Change Service. 2025. Copernicus: 2024 is the first year to exceed 1.5°C above pre-industrial level, *https://climate.copernicus.eu/*. Online: https://climate.copernicus.eu/copernicus-2024-first-year-exceed-15degc-above-pre-industrial-level, accessed on January 30, 2025.

[2] European Commission. 2020. Communication from the commission to the European parliament, the council, the European economic and social committee and the committee of the regions; Stepping up Europe's 2030 climate ambition; Investing in a climate-neutral future for the benefit of our people. *COM(2020) 562 final*, Brussels, Belgium.

[3] European Commission. 2024. Recommendation for 2040 target to reach climate neutrality by 2050, *https://commission.europa.eu/*. Online: https://commission.europa.eu/news/recommendations-2040-targets-reach-climate-neutrality-2050-2024-02-06_en, accessed on January 6, 2025.

[4] Ruprecht, D., Schmidt-Achert, T., Zahler, J., Pichlmaier, S. 2022. Imports of green hydrogen and its derivatives to Germany in a climate neutral future. Publisher: Forschungsstelle für Energiewirtschaft e.V.

[5] IRENA (2022), Global hydrogen trade to meet the 1.5°C climate goal: Part I – Trade outlook for 2050 and way forward, International Renewable Energy Agency, Abu Dhabi.

[6] Smith, J., Mastorakos, E. A Systems-Level Study of Ammonia and Hydrogen for Maritime Transport, Maritime Transport Research, Volume 5, 2023, 100099, ISSN 2666-822X, https://doi.org/10.1016/j.martra.2023.100099.

[7] Wendlinger, C., Kigle, S., Ebner, M., Neitz-Regett, A., Pichlmaier, S. 2022. Wasserstofftransportoptionen. *https://www.ffe.de/veroeffentlichungen/wasserstofftransport-analyse-der-prozessketten-kostenbewertung-und-gegenueberstellender-vergleich/*, accessed on February 9, 2025.

[8] Menefee, A., Schwartz, B. 2024. Comparing green hydrogen and green ammonia as energy carriers in utility-scale transport and subsurface storage, Energy and Climate Change, Volume 5, 2024, 100163, ISSN 2666-2787, https://doi.org/10.1016/j.egycc.2024.100163.

[9] DEA, The technology catalogues of the Danish energy agency, https://ens.dk/service/fremskrivninger-analyser-modeller/teknologikataloger, 2022.

[10] Forschungsradar: Metaanalyse: Die Rolle erneuerbarer Gase in der Energiewende, 2018.

[11] IRENA and AEA. 2022. *Innovation Outlook: Renewable Ammonia*, International Renewable Energy Agency, Abu Dhabi, Ammonia Energy Association, Brooklyn

[12] Ammonia as a marine fuel, https://en.nabu.de/imperia/md/content/nabude/verkehr/210622-nabu-study-ammonia-marine-fuel.pdf, accessed on January 21, 2024.

[13] https://webbook.nist.gov/cgi/cbook.cgi?ID=C7664417&Mask=1

[14] Trangwachirachai, K., Rouwenhorst, K., Lefferts, L., Faria Albanese, J. 2024. Recent progress on ammonia cracking technologies for scalable hydrogen production, *Current* Opinion in Green and Sustainable Chemistry, Volume 49, DOI: 10.0945.

[15] Alboshmina, N. 2019. Ammonia cracking with heat transfer improvement technology. Doctoral thesis. Cardiff University, UK.

[16] A. Valera-Medina, F. Amer-Hatem, A. K. Azad, I. C. Dedoussi, M. de Joannon, R. X. Fernandes, P. Glarborg, H. Hashemi, X. He, S. Mashruk, J. McGowan, C. Mounaïm-Rouselle, A. Ortiz-Prado, A. Ortiz-Valera, I. Rossetti, B. Shu, M. Yehia, H. Xiao, M. Costa, Energy & Fuels, DOI: 10.1021/acs.energyfuels.0c03685.

[17] G. Pirker, M. Klawitter, A. Ramachandran, C. Gößnitzer, A. Tilz, A. Wimmer, Characterization of future fuels using an optically accessible rapid compression machine, presented at 30th CIMAC World Congress 2023: Meeting the Future of Combustion Engines, Busan, June, 2023.

[18] Plass, J., Tietz, C. Steffen, M. Engelmeier, L., Zinnemann, M., Nickig, N. 2024. Modellierung des dynamischen Betriebs einer Ammoniak-Crackeranlage für die Versorgung von Ammoniakmotoren unter Einbeziehung eines 2D-FVM-Reaktormodell, *AVL Simulation Conference*, Regensburg, Germany.

[19] Meléndez Rey, J., Antonio Medrano, J. 2024. Ammonia Cracking in membrane reactors for high purity hydrogen production, Ammonia Energy Association. https://ammoniaenergy.org/wp-content/uploads/2024/05/Ammonia-Project-Features-speaker-slides-May-2024.pdf

[20] J. B. Heywood, Internal combustion engine fundamentals, McGraw-Hill Education, New York City, NY, USA 2018.

[21] F.R. Westlye, A. Ivarsson, J. Schramm, Fuel, DOI: 10.1016/j.fuel.2013.03.055.

[22] A. Yousefi, H. Guo, S. Dev, B. Liko, S. Lafrance, Fuel, DOI: 10.1016/j.fuel.2021.122723.

[23] G.-W. Lee, B.-H. Shon, J.-G. Yoo, J.-H. Jung, K.-J. Oh, Journal of Industrial and Engineering Chemistry, DOI: 10.1016/j.jiec.2008.02.013.

[24] M. Meffert, D. Lenane, M. Openshaw, J. Roos, SAE Technical Paper, DOI: 10.4271/2000-01-1952.

[25] IPCC, The Earth's Energy Budget, Climate Feedbacks, and Climate Sensitivity. In Climate Change 2021: The Physical Science Basis. Contribution of Working Group I to the Sixth Assessment Report of the Intergovernmental Panel on Climate Change", https://www.ipcc.ch/report/ar6/wg1/, accessed: July, 2023.

[26] Wermuth, N., Lackner, M., Kammel, G., Malin, M., Wimmer, A., Url, M., & Spyra, N. (2024). Potential and limitations of different hydrogen combustion concepts for power generation applications. In WTZ Roßlau GmbH (Ed.), Tagungsband 13. Dessauer Gasmotoren-Konferenz (pp. 164 - 175). FVTR Forschungszentrum für Verbrennungsmotoren und Thermodynamik Rostock GmbH.

[27] M. Coppo, N. Wermuth, 2022. Powering a greener future: the OMT injector enables high-pressure direct injection of ammonia and methanol, pp. 68-81, Proceedings of the 7th RGMT, Rostock, Germany.

10 CONTACT

Univ.-Prof. Dr.-Ing. Nicole Wermuth
Institute of Thermodynamics and Sustainable Propulsion Systems, Research Area
"High Performance Large Engine Systems"
Inffeldgasse 19, 8010 Graz, Austria
Email: nicole.wermuth@ivt.tugraz.at
Phone: +43 316 873-30087